DTIC
ENI.
4 86

MICROCOPY RESOLUTION TEST CHART
NATIONAL BUREAU OF STANDARDS-1963-A

MOLECULAR JET STUDY OF THE SOLVATION OF BENZENE BY

METHANE, ETHANE, AND PROPANE

by

Mark Schauer and E.R. Bernstein
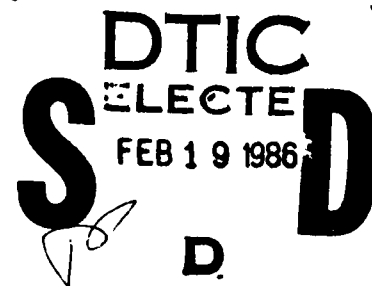
Department of Chemistry
Colorado State University
Fort Collins, Colorado  80523

January 15, 1985

AD-A164 556

DTIC
SELECTE
FEB 1 9 1986
S
D
D

DTIC FILE COPY

86  2  19    005

| REPORT DOCUMENTATION PAGE | | READ INSTRUCTIONS BEFORE COMPLETING FORM |
|---|---|---|
| 1. REPORT NUMBER<br>Technical Report #14 | 2. GOVT ACCESSION NO.<br>-1) -1 /6 4 | 3. RECIPIENT'S CATALOG NUMBER<br>556 |
| 4. TITLE (and Subtitle)<br>Molecular Jet Study of the Solvation of Benzene by Methane, Ethane, and Propane | | 5. TYPE OF REPORT & PERIOD COVERED<br>Technical Report |
| | | 6. PERFORMING ORG. REPORT NUMBER |
| 7. AUTHOR(s)<br>Mark Schauer and E.R. Bernstein | | 8. CONTRACT OR GRANT NUMBER(s)<br>N00014-79-C-0647 |
| 9. PERFORMING ORGANIZATION NAME AND ADDRESS<br>Colorado State University<br>Department of Chemistry<br>Fort Collins, CO 80523 | | 10. PROGRAM ELEMENT, PROJECT, TASK AREA & WORK UNIT NUMBERS |
| 11. CONTROLLING OFFICE NAME AND ADDRESS<br>Chemistry Program, Materials and Science Division<br>Office of Naval Research, 800 N. Quincy Street<br>Arlington, Virginia 22217 | | 12. REPORT DATE<br>January 15, 1985 |
| | | 13. NUMBER OF PAGES<br>47 |
| 14. MONITORING AGENCY NAME & ADDRESS(if different from Controlling Office) | | 15. SECURITY CLASS. (of this report)<br><br>Unclassified |
| | | 15a. DECLASSIFICATION/DOWNGRADING SCHEDULE |

16. DISTRIBUTION STATEMENT (of this Report)

This document has been approved for public release and sale; its distribution is unlimited.

17. DISTRIBUTION STATEMENT (of the abstract entered in Block 20, if different from Report)

18. SUPPLEMENTARY NOTES

19. KEY WORDS (Continue on reverse side if necessary and identify by block number)

20. ABSTRACT (Continue on reverse side if necessary and identify by block number)

Two color time of flight mass spectroscopy studies of benzene solvated by methane, ethane, and propane in a molecular jet has been carried out. Absorption has been characterized for both the $0^0_0$ and $6^1_0$ transitions of benzene (alkane)$_x$(X=1,2,3...). Atom-atom exponential-6 potentials have been employed to calculate cluster geometry and binding energy. Comparisons between calculations and experiments allow the identification of specific configurations for the cluster spectroscopic transitions. Cluster spectral shifts can also be identified and a correlation between the size of the cluster red shift and geometry

**DD** FORM 1473 EDITION OF 1 NOV 65 IS OBSOLETE
1 JAN 73

20. has been developed. The closer the solvent is to the aromatic $\pi$ system of the ring, the larger the red shift. Relative intensity data for different clusters has led to a clarification of cluster nucleation. Most clusters are formed by the interaction of solvent dimers or larger species with a solute molecule.

## I. INTRODUCTION

Supersonic molecular jet expansions are known to produce a rich array of van der Waals (vdW) clusters in an environment accessible to various spectroscopic techniques.[1] Photoionization time of flight mass spectroscopy (TOFMS) is especially useful for the deconvolution of the absorption spectra of various clusters in the beam[2]. The study of large clusters can be carried out with this relatively easy mass selective technique and thereby the modeling of condensed phases and aggregated systems can be explored. Furthermore, the evolution of the mass detected absorption spectrum of a central chromophore as larger clusters are observed provides some insight into nucleation processes and intermolecular interactions in condensed phases.

One readily attainable spectroscopic parameter which can be of help in characterizing a cluster is the spectral shift for a given transition; that is, the difference in energy between a cluster vibronic feature and the comparable feature in the isolated solute molecule. It is found that in the case of benzene solvated with methane, ethane, or propane, the spectral shift depends essentially on the cluster geometry. The general geometries of most of the small clusters can be deduced from the qualitative analysis of the patterns and trends of the spectral shifts, from vdW vibronic features, and by analogy with other systems for which the geometry is known.[3] For many clusters, additional information is necessary to deduce cluster

- 1 -

geometry. One approach is to use high resolution spectroscopy to obtain the rotational spectra of these clusters.[3,4] Aside from being technically difficult, this approach usually will not yield detailed enough information to reveal the exact structures of larger clusters. A simpler and potentially more useful approach to finding the geometries of larger clusters is to use computer modeling of the clusters to calculate minimum energy configurations.[5] If the low energy configurations of a given cluster are consistent with spectroscopic data for the system, the spectroscopic features of a particular geometry can be identified. The assignments help to elucidate the complicated relationship between geometry and spectral shift.

The assignment of spectral features to specific geometries also provides insight into the nucleation process in the jet. Solvent molecules may add to benzene one molecule per collision, a process we will call homogeneous nucleation, or a benzene molecule may bind to a solvent cluster to add more than one molecule per collision. This latter inhomogeneous nucleation typically results in very anisotropic clusters - clusters in which most of the solvent molecules are on one side of the ring. Homogeneous nucleation can produce relatively isotropic clusters which may be thought of as model liquid solution or matrix systems.[6] However, inhomogeneous nucleation seems to predominate in the formation of the larger clusters in this study.

- 2 -

This report will present the spectroscopic results of the study of benzene clustered with methane, ethane and propane $\left(Ben(CH_4)_x, Ben(C_2H_6)_x, Ben(C_3H_8)_x\right)$ together with the results of computer modeling of the clusters. Attention will be confined in this paper to small clusters $(x \leq 3)$. In a companion paper [7] (hereafter referred to as II) the results for toluene clustered with methane, ethane, and propane will be presented. The differences and similarities between benzene clusters and toluene clusters will be discussed in II.

## II EXPERIMENTAL PROCEDURES

The apparatus and techniques employed in this study are largely the same as those previously reported.[8] Fluorescence excitation experiments were found to be of limited utility as the clusters of interest are nearly always minority species in the beam. In addition, dispersed emission from most of the clusters is weak and complicated as noted previously.[9] Consequently, only mass selective absorption spectra (2-color TOFMS)[8,9] will be discussed in this paper.

The optimum nozzle backing pressure is the same for all spectra reported in this work $(P_o \sim 100$ psi$)$ and the nozzle is kept at ca. 300K throughout these experiments. The concentration of solvent in the backing region for all systems discussed is 2%. Dispite nearly identical backing conditions throughout, intensity comparisons between species are difficult. The various solvents cluster differently and a particular expansion condition can produce different concentrations of multimers for different solvents.

- 3 -

Other changes have been made in the previously reported experimental conditions. A Comlinear Corp CLC 100 linear amplifier is placed directly after the ion detector as required to enhance the weakest signals by a factor of 10. The viton O-ring which seals the pulsed nozzle has been replaced by a Teflon coated viton O-ring to prevent swelling of the O-ring due to absorption of benzene.

Finally, a cost savings of about $20/10 hours of laser operation time can be realized by recycling the coumarin 500 laser dye. Most of the undecomposed dye can be recovered from the batch of used dye (which lasts about 20 hours) by a single recrystallization from methanol and water. Slow evaporation of a dye-methanol solution produces good quality dye crystals: no reduction in performance is noted for recycled dye.

The calculation of cluster energy is performed on an HP 9845 desktop computer. An atom - atom (exp-6) intermolecular potential of the form

$$E_{ij} = -\frac{A_{ij}}{R_{ij}^6} + B_{ij} \exp[-C_{ij}R_{ij}]$$

is employed in which A, B and C are parameters and $R_{ij}$ is the distance between the $i^{th}$ and $j^{th}$ atoms of different molecules. Summing over all pairs of atoms on different molecules gives the total intermolecular energy of the cluster.

Parameters used in these calculations are adapted from those given in the literature.[10,11] Parameters determined for methane are used for all of the solvents. The values used are given in Table I.

The minimization routine to find the minimum energy configurations involves moving one solvent molecule at a time a step in each of the translational and each of the three rotational degrees of freedom. The new energy of the cluster is calculated and compared to the previous energy. If the new energy is lower, the step is repeated; if it is not lower, the next degree of freedom is tried. Although simple, this technique cannot guarantee that the absolute minimum energy configuration has been found. Consequently, local minima in the potential energy surface are often found and one must be careful to sample all of configuration space to be certain that the lowest energy configuration has indeed been located. Often intuition developed through the study of simpler systems can limit the number of possible initial configurations that must be sampled.

The calculated binding energy is the depth of the ground state vdW potential well ($D_e{}''$). The measured binding energies are $D_o{}'$. The difference between these values includes ground and excited state energy differences (cluster spectral shifts) and zero point energies. Considering the accuracies of the experiments and the calculations, these differences are at present neglected in the discussion.

## III  RESULTS

The allowed $6_0^1$ transition of benzene is intense in all of the clusters and is relatively free of influence from other transitions. The spectra of the various clusters are easily assigned in this region. The $0_0^0$ region was also scanned for each of the clusters: only clusters with symmetry lower than $C_3$ will exhibit a $0_0^0$ origin peak. The presence or absence of the $0_0^0$ feature of a cluster helps to identify the cluster geometry. While vibronic transitions higher

- 5 -

than $6_0^1$ of benzene are observed, no higher transitions of the

clusters are reported because of congestion and low intensity of the

cluster spectra.

The assignments for vdW vibrational features given below are

made to be consistent with previous assignments of the aniline-

methane,[6] and toluene-methane[9] systems and with assignments given in

II. In all of these systems the frequencies of the symmetric vdW

stretches scale appropriately with the masses and force constants

(binding energies). The vdW bending modes are typically lower in

energy and intensity than the stretches. Using these general

guidelines the assignments given below are reasonable and fit well

into the previous patterns of vdW mode frequencies.

Benzene-Methane

The $6_0^1$ transition of $Ben(CH_4)_1$ is shifted $-41 cm^{-1}$ from

the benzene $6_0^1$ (see figure 1 and Table II). A progression in the

vdW stretch is observed with a stretching frequency of $32 cm^{-1}$. In

addition a vdW bend with a frequency of $27 cm^{-1}$ is seen. The $0_0^0$

of $Ben(CH_4)_1$ is not observed, indicating that the 3-fold axis of

benzene is preserved in the $Ben(CH_4)_1$ cluster.

$Ben(CH_4)_2$ at $6_0^1$ reveals two configurations (see figure 1,

Table II). Configuration I has a spectral shift of $-81 cm^{-1}$: twice

that of $Ben(CH_4)_1$. A symmetric stretch with a frequency of $31 cm^{-1}$

is noted. Configuration II of $Ben(CH_4)_2$ evidences a $-40 cm^{-1}$

spectral shift: this feature is broader than those of configuration

I.

In the region of the $Ben(CH_4)_2$ $0_0^0$ only one peak with a spectral shift of $-40$ $cm^{-1}$ is observed (see figure 2): therefore, configuration I of $Ben(CH_4)_2$ preserves the 3-fold axis of benzene and configuration II does not.

The geometries of $Ben(CH_4)_{1,2}$ can, to a large extent, be deduced from the spectra. In $Ben(CH_4)_1$ the methane must rest symmetrically above the ring to preserve the 3-fold axis of benzene. Configuration I of $Ben(CH_4)_2$ must have methane symmetrically above and below the benzene ring, and configuration II must have both methanes on the same side of the ring to produce an asymmetric geometry with a non-additive shift and an induced $0_0^0$ transition.

The computer modeling of these two clusters agrees perfectly with the geometries deduced from the spectra (see figure 3, Table III). The minimium energy configuration of $Ben(CH_4)_1$ preserves the 3-fold axis of benzene. The predicted binding energy is 599 $cm^{-1}$; a value greater than 522 $cm^{-1}$ as required if the $6_0^1$ is to be observed for $Ben(CH_4)_1$. Two configurations for $Ben(CH_4)_2$ arise from the computer modeling. One preserves the 3-fold axis of benzene and should have a spectral shift twice that of $Ben(CH_4)_1$, and the other configuration is asymmetric with both methanes on the same side of the ring.

The spectrum of $Ben(CH_4)_3$ evidences two configurations also. Configuration I has a shift similar to configuration I of $Ben(CH_4)_2$ (see figure 1). This geometry probably consists of $Ben(CH_4)_2$ configuration II with a methane bound symmetrically below the ring for

a total shift of about $-80$ cm$^{-1}$. The other configuration of Ben(CH$_4$)$_3$ probably features all three methanes on the same side of the ring to produce a small ($-40$ cm$^{-1}$) spectral shift. The peaks in the Ben(CH$_4$)$_3$ spectrum are more diffuse than those of Ben (CH$_4$)$_{1,2}$ indicating that a number of slightly different configurations probably exist. The Ben(CH$_4$)$_3$ $6_0^1$ spectrum is sufficiently weak that the $0_0^0$ is not to be expected. Calculations were not done for this cluster.

Benzene-Ethane

Ben(C$_2$H$_6$)$_1$ shows two different configurations in the $6_0^1$ region (see figure 4, Table IV). Configuration I has a spectral shift of $-57$ cm$^{-1}$ and a long, regular progression in the vdW stretch with a frequency of 17 cm$^{-1}$. Configuration II has a shift of $-51$ cm$^{-1}$ and a stretching frequency of 16 cm$^{-1}$. The spectrum of Ben(C$_2$H$_6$)$_1$ at the $0_0^0$ (see figure 5, Table V) exhibits only the origin associated with configuration II and two associated vdW bends. The relative intensity of the bends is much larger at the origin than at $6_0^1$; the vdW stretch is not evident at the origin, perhaps due to the similarity of the ground and excited state potentials.

The Ben(C$_2$H$_6$)$_2$ (see figure 4, Table II) configuration I has a spectral shift of $-53$ cm$^{-1}$, at $6_0^1$ and is not seen at the $0_0^0$. Configuration II of this species reveals a spectral shift of $-48$ cm$^{-1}$, a stretching frequency of 18 cm$^{-1}$, and one bending mode in the $6_0^1$ region. At the origin, only the $0_0^0$ of configuration II is found with its associated vdW bends (see figure 5, Table V); again, no stretches are observed.

- 8 -

The calculations for $Ben(C_2H_6)_1$ agree quite nicely with the spectra (see figure 6, Table VI). Two configurations of minimum energy are found: one which preserves the 3-fold axis of benzene and one which does not. The asymmetric configuration is predicted to have a 120 $cm^{-1}$ larger binding energy.

The computer modeling of $Ben(C_2H_6)_2$ reveals several stable geometries two of which are presented in figure 7 and Table VII. All geometries involving an ethane on either side of the ring must be dismissed since the spectrum of $Ben(C_2H_6)_2$ in the region of $6_0^1$ shows no configurations with an additive spectral shift with respect to $Ben(C_2H_6)_1$. Only one geometry (labeled 1 in figure 7) is found in the computer modeling which preserves the 3-fold axis of benzene. Several other geometries of $Ben(C_2H_6)_2$, which should have spectral shifts similar to that found for configuration II (see figure 4), are predicted in the computer modeling of $Ben(C_2H_6)_2$. The most stable of these is shown in figure 7.

Benzene-Propane

Only one configuration of $Ben(C_3H_8)_1$ is clearly evident from the spectrum (figure 8, Table VIII). The $6_0^1$ peak of this cluster is shifted -72 $cm^{-1}$ from the monomer $6_0^1$. An intense progression in the stretch is evident with a frequency of 24 $cm^{-1}$. The unassigned peak -57 $cm^{-1}$ from the monomer $6_0^1$ may be due to a different configuration, or it may be due to some high frequency vdW motion. No $0_0^0$ peak is observed for this cluster indicating that the cluster geometry preserves the 3-fold axis of benzene.

- 9 -

The vdW stretch of $Ben(C_3H_8)_1$ seems to have a positive anharmonicity for the first two quanta of the stretch. Underlying peaks due to slightly different configurations could be modifying the lineshapes of some of the peaks to produce this effect. It is difficult to envision how the symmetric stretch of the cluster could have a positive anharmonicity; however, this possibility cannot be dismissed. A similar but much less pronounced effect is observed for the stretch of $Ben(C_2H_6)_1$.

There is no peak in the $Ben(C_3H_8)_2$ $6_0^1$ spectrum with a shift twice that of $Ben(C_3H_8)_1$. One configuration of $Ben(C_3H_8)_2$ seen in the $6_0^1$ region has a spectral shift of $-83$ $cm^{-1}$, and a stretching frequency of $23$ $cm^{-1}$. Other geometries with smaller spectral shifts are observed. No peaks are observed at the cluster $0_0^0$ position.

The computer modeling of $Ben(C_3H_8)_1$ shows several possible configurations. The lowest energy configuration possesses the highest symmetry and is pictured in figure 9 (see Table IX). The three hydrogen atoms closest to the ring are positioned almost symmetrically above the ring. The $0_0^0$ transition of $Ben(C_3H_8)_1$ is not observed presumably due to the approximate three-fold symmetry of this cluster. The spectrum of $Ben(C_3H_8)_2$ does not show an origin either. One example of a $Ben(C_3H_8)_2$ cluster which preserves this local symmetry is pictured in figure 9. Other similar configurations are possible.

The spectrum of $Ben(C_3H_8)_3$ in the $6_0^1$ region indicates that at least two configurations of this cluster exist (see figure 10, Table X). Due to the small spectral shifts, the clusters must involve all 3 solvent molecules situated above the ring. The cluster $0_0^0$ transitions with associated vdW bends are seen for both of these configurations. No calculations were performed on these clusters.

## IV  DISCUSSION

The ability to assign geometries to clusters giving rise to certain peaks in the spectra leads to a greater understanding of both the energetics of the system and the process of cluster formation. The relationships between geometry and spectral shift will be explored first, followed by a discussion of the nucleation processes in the jet.

### Spectral Shift

The spectral shift for a cluster is the difference between the cluster binding energy in the ground and excited states. The shift depends on the polarizability of the solvent along the intermolecular bond and on the change in polarizability of the solute upon excitation in the region (direction) of this bond. The solute polarizability may change quite differently for different binding sites on benzene to produce different spectral shifts for different geometries.

The spectra of $Ben(CH_4)_{1,2}$ (see figure 1) demonstrate that binding of a methane symmetrically above or below the aromatic ring contributes about $-40$ $cm^{-1}$ to the spectral shift of the complex. However, the asymmetric binding of two methanes above the ring (yielding an observed $0_0^0$ transition) produces a shift of only $-40$ $cm^{-1}$. The computer modeling of the asymmetric $Ben(CH_4)_2$ cluster shows that one of the methanes is largely above the ring (although displaced from the center by .695 $\overset{o}{A}$) while the other methane is displaced by 2.778 $\overset{o}{A}$ from the ring center. This latter $CH_4$ is above the midpoint of the C-H bond (see figure 3 and Table 3). If this geometry is correct, almost all of the spectral shift of this cluster must be due to the interaction of benzene with the methane above the

ring. The other methane must contribute virtually nothing to the spectral shift even though it is bound nearly as tightly to benzene. In fact, the asymmetric (II) $Ben(CH_4)_2$ cluster has a virtually identical binding energy, but a much smaller spectral shift, than the symmetric $Ben(CH_4)_2$ cluster.

These observations lead to the conclusion that interaction of the solvent with the aromatic $\pi$-cloud of benzene is responsible for most of the spectral shift even though the binding energy may be nearly as large for other binding sites. Such a generalization helps to explain the spectral shifts of other clusters as well

The spectral shifts of the two distinct (symmetric and asymmetric) geometries of $Ben(C_2H_6)_1$ are deduced and assigned in the Results section. The higher symmetry cluster (figure 6), which preserves the three-fold axis of benzene, has a larger spectral shift than the lower symmetry cluster for which the origin is observed. As in the benzene-methane system, the calculated binding energies for the two configurations are virtually identical, yet the asymmetric configuration has a much smaller spectral shift.

Apparently, both orientation and position of a solvent molecule play an important role in determining the spectral shift and binding energy of a cluster of given composition. Ethane has a larger polarizability parallel to its long axis than perpendicular to it.[12] Therefore the orientation of the long axis of ethane with respect to the plane of the benzene ring, and the position of the center of the ethane molecule with respect to the center of the benzene ring have considerable effect on both spectral shifts and binding energies. The

- 12 -

larger spectral shift is associated with the solute-solvent relative orientation for which the direction of large solvent polarizability is perpendicular to the plane of the ring, directly over the center of the molecular system. The asymmetric configuration (II) of $Ben(C_2H_6)_1$ has a larger calculated binding energy (-778 vs. -654 $cm^{-1}$) and a smaller shift (-51 vs. -57 $cm^{-1}$) most likely arising from a reduced $\pi$-system interaction but a larger overall benzene-ethane interaction: in this configuration the ethane long axis is nearly parallel to the plane of the benzene ring. Ethane in these two different orientations interacts with benzene as though it were two different solvents with different sizes and polarizabilities.

The spectral shifts for the two configurations of $Ben(C_2H_6)_2$ are nearly identical to the shifts for the $Ben(C_2H_6)_1$ configurations. Based on the calculations, the geometries for $Ben(C_2H_6)_2$ involve $Ben(C_2H_6)_1$ structures with a second $C_2H_6$ coordinated on the same side of the ring as the first $C_2H_6$ group: the amount of solvent $\pi$-cloud overlap is about the same in $Ben(C_2H_6)_2$ as in $Ben(C_2H_6)_1$.

The calculated geometry of $Ben(C_3H_8)_1$ which agrees with the spectroscopic data (i.e. no $0_0^0$ transition, large spectral shift) features a large interaction between the propane and the $\pi$-system of benzene. The calculated configuration is depicted in figure 9: this arrangement of solute and solvent has approximate high symmetry with all three carbon atoms lying near th aromatic $\pi$-system. The binding energies and shifts for the $Ben(C_3H_8)_2$ clusters are also consistent with the above conclusions.

- 13 -

## The Nucleation Process

The relative intensities of the features of various cluster geometries can reveal something of the nucleation processes in the molecular jet. The $Ben(S)_2$ data are particularly useful in focusing on these processes. In general, two geometries can exist for this complex: a solvent molecule can be on either side of the ring (isotropic cluster) or both solvent molecules can be on the same side of the ring (anisotropic cluster). Although homogeneous nucleation can conceivably create either type of cluster, inhomogeneous nucleation can only create anisotropic clusters of this size. By examining the relative intensities of the spectral features of each type of cluster, one can determine the relative concentration of isotropic vs. anisotropic clusters in the jet. In this way the nucleation processes in the jet can be elucidated.

The spectra of $Ben(C_2H_6)_2$ and $Ben(C_3H_8)_2$ (figures 4 and 8) show that there are virtually no isotropic clusters of these species. Since homogeneous nucleation should produce both isotropic and anisotropic clusters, inhomogeneous nucleation appears to be the dominant nucleation process for these systems under the present beam conditions. By contrast, the $Ben(CH_4)_2$ spectrum (figure 1) shows both isotropic and anisotropic clusters in roughly equal numbers. Therefore, homogeneous nucleation does occur for the benzene-methane system.

The lack of homogeneous nucleation in $Ben(C_2H_6)_2$ and $Ben(C_3H_8)_2$ indicates that the number of solvent monomers relative to dimers and larger solvent clusters is probably small for ethane and propane solvents. However, based on the calculated binding energies the relative number of methane monomers should also be small.

Therefore, it is unlikely that enough methane monomers exist in the beam to explain the amount of homogeneous nucleation observed for $Ben(CH_4)_2$.

It is difficult to get data on the relative concentrations of molecular clusters in a jet expansion, especially for the hydrocarbon systems. Some data are available on the concentration of dimers relative to monomers for ethylene under rather modest expansion conditions. ($P_o$= 5 -10 atm, d = 35 $\mu$m orifice).[13] The apparent ratio of monomers to dimers is roughly 4:1 for these conditions: The relative concentration of clusters scales with ($P_o^2$d) and thus our expansion conditions will produce a factor of 15 higher concentration of clusters. The observed 4:1 ratio for ethylene is, however, heavily distorted by fragmentation caused by the electron impact ionization technique: for example, almost all observed dimers arise from higher clusters. Hence, the actual ratio of monomer to dimer neutrals is not well estimated by those methods; dimer and higher clusters could easily dominate the distribution of species in their expansion and most certainly dominate under our more extreme expansion conditions.

If the homogeneous nucleation of $Ben(CH_4)_2$ is not occuring through the interactions of methane monomers and benzene (and a third body to carry off the binding energy)[14], this nucleation must be occuring through the interaction of dimers (or larger clusters) with benzene. Upon interaction with benzene, the methane dimer can dissipate part of the binding energy through vibrational predissociation (VP). This interactive collision leaves one methane bound to benzene while the other methane carries off a portion of the excess binding energy.

The binding energies of the solvent dimers, as well as those

- 15 -

for benzene with the three solvents, are given in Table XI. The values are derived from computer modeling of the clusters. The data suggest that only about half of the binding energy of a solvent to benzene can be dissipated through VP of the solvent dimer.

If the binding energy does not cause VP of the solvent dimer before a third body interacts with the complex and carries away the excess binding energy, the resultant clusters will be anisotropic. Therefore, the nucleation of benzene with ethane and propane is inhomogeneous because the solvent dimers do not undergo VP quickly enough during the collision/formation process.

Based on the above reasoning, one would expect that a large solute-solvent binding energy would result in an increased number of homogenously nucleated (isotropic) clusters. Evidence is presented in II for the toluene-solvent systems which support this conclusion.

V. CONCLUSIONS

Two-color TOFMS studies have been employed to determine the general geometry and symmetry of small benzene-hydrocarbon clusters: comparison of cluster $0_0^0$ and $6_0^1$ transitions makes possible the experimental identification of cluster geometry (symmetry) with spectral shift and vibrational features. Through computer modeling of van der Waals clusters of benzene and small hydrocarbons, a correlation between detailed cluster geometry and spectral features has proven possible. The specific assignments lead to a general pattern for the relationship between geometry and spectral shift. The spectral shift in these systems seems to be largely due to the interaction of the solvent with the aromatic $\pi$-electron system of

- 16 -

benzene. This would explain the observations that spectral shift and calculated binding energy are not directly related. Of course, the details of these calculations are a function of the model chosen for the potential (atom - atom exp-6).

The assignment of geometry to clusters with a specific spectral shift has also made possible a better understanding of the nucleation processes in the jet. We suggest that due to the relatively low concentration of solvent monomers in the system, homogeneous nucleation can occur through the VP of solvent dimers as the dimers interact with benzene. If the binding energy of the solvent dimer is not small relative to the solute-solvent binding energy, VP will not occur and anisotropic geometries of the solute-solvent clusters will comprise the major cluster species in the beam.

ACKNOWLEDGEMENT

# REFERENCES

1) D.H. Levy, L. Wharton and R.E. Smalley, Chemical and Biochemical Applications of Lasers, (Academic Press, NewYork, 1977), Vol. II, pp. 1-41.

2) J.B. Hopkins, D.E. Powers and R.E. Smalley, J. Phys. Chem. 85, 3739 (1981).

3) S.M. Beck, M.G. Liverman, L.L. Monts, and R.E. Smalley, J. Chem. Phys., 70, 232 (1979).

4) R.E. Smalley, L. Wharton, D.H. Levy, and D.W. Chandler, J. Chem. Phys., 68, 2487 (1978).

5) M.J. Ondrechen, Z. Berkovitch-Yellin and J. Jortner, J. Am. Chem. Soc., 103, 6586 (1981).

6) See for example: E.R. Bernstein, K. Law and Mark Schauer, J. Chem. Phys., 80, 634 (1984) and references therein.

7) Mark Schauer, K. Law, E.R. Bernstein, J. Chem. Phys. following paper.

8) E.R. Bernstein, K. Law and Mark Schauer, J. Chem. Phys. 80, 207 (1984).

9) Mark Schauer, K. Law and E.R. Bernstein, J. Chem. Phys., 81, 49 (1984).

10) D.E. Williams, J. Chem. Phys. 45, 3770 (1966).

11) H. Yasuda, J. Chem. Phys. 73, 3722 (1980).

12) D.W. Davies, Mol. Phys. 17, 473 (1969).

13) M.P. Casassa, D.S. Bomse and K.C. Janda, J. Chem. Phys 74, 5044 (1981).

14) O.F. Hagena, Molecular Beams and Low Density Gasdynamics, (Marcel Dekker, Inc)., New York, 1974), Vol. 4, pp. 93-181.

TABLE I

Parameters for the energy expression in the computer modeling of the vdW clusters.
of Benzene.

$$E_{ij} = - A_{ij} \Big/ R_{ij}^6 + B_{ij} \exp [ - C_{ij} R_{ij}]$$

$$A(\frac{cm^{-1} \cdot \mathring{A}^6}{mole}) \quad B(\frac{cm^{-1}}{mole}) \quad C \ (\mathring{A}^{-1})$$

Aliphatic-Aliphatic[a]

|     |        |          |        |
| --- | ------ | -------- | ------ |
| C-C | 131096 | 8890353  | 3.421  |
| C-H | 47830  | 7562708  | 3.94   |
| H-H | 15028  | 6390528  | 4.643  |

Aliphatic-Aromatic[b]

|     |        |          |        |
| --- | ------ | -------- | ------ |
| C-C | 162645 | 16520286 | 3.5105 |
| C-H | 47864  | 6434085  | 3.805  |
| H-H | 13071  | 2497533  | 4.1915 |

Aromatic-Aromatic[c]

|     |        |          |        |
| --- | ------ | -------- | ------ |
| C-C | 201786 | 30698427 | 3.6    |
| C-H | 47897  | 5473891  | 3.67   |
| H-H | 11368  | 976084   | 3.74   |

a) From the methane-methane parameters of ref. 11

b) The parameters are found by combining the benzene-benzene and methane-methane parameters as follows:

$$A_{Bm} = (A_{BB} A_{mm})^{\frac{1}{2}}$$

$$B_{Bm} = (B_{BB} B_{mm})^{\frac{1}{2}}$$

$$C_{Bm} = \frac{1}{2}(C_{BB} + C_{mm})$$

c) From the benzene-benzene parameters of ref. 10

TABLE II

The prominent peaks in the spectra of $Ben(CH_4)_1$ and $Ben(CH_4)_2$ in the region of $6_0^1$ (see figure 2).

| Species | Energy (vac cm$^{-1}$) | Energy relative To Ben $6_0^1$ (cm$^{-1}$) | Energy relative To cluster $6_0^1$ | Assignment[a] |
|---|---|---|---|---|
| $Ben(CH_4)_1$ | 38567.6 | -41 | 0 | $6_0^1$ |
| | 38594.6 | | 27.3 | $6_0^1 B_0^1$ |
| | 38599.9 | | 32.3 | $6_0^1 V_0^1$ |
| | 38619.0 | | 51.4 | $6_0^1 V_0^2$ |
| $Ben(CH_4)_2$ | 38527.1 | -81.4 | 0 | I $6_0^1$ |
| | 38557.1 | | 30.6 | I $6_0^1 V_0^1$ |
| | 38568.1 | -40.4 | 0 | II $6_0^1$ |

a) B stands for a vdW bend and V stands for the vdW stretch. I and II represent different configurations.

TABLE III

The atomic positions for the minimum energy configurations of
$Ben(CH_4)_1$ and $Ben(CH_4)_2$ (see figure 3). Coordinates are in $\overset{o}{A}$ with the origin
at the center of benzene. the X axis passes through a carbon atom on the
benzene, the Y axis bisects a C-C bond on benzene and the Z axis is coincident
with the 6-fold symmetry axis of benzene.

| | Atom | X($\overset{o}{A}$) | Y($\overset{o}{A}$) | Z($\overset{o}{A}$) | Energy $(cm^{-1})$ |
|---|---|---|---|---|---|
| Benzene | | | | | |
| | C1 | -1.395 | 0 | 0 | |
| | C2 | - .6975 | 1.208 | 0 | |
| | C3 | .6975 | 1.208 | 0 | |
| | C4 | 1.395 | 0 | 0 | |
| | C5 | .6975 | -1.208 | 0 | |
| | C6 | - .6975 | -1.208 | 0 | |
| | H1 | -2.479 | 0 | 0 | |
| | H2 | -1.24 | 2.147 | 0 | |
| | H3 | 1.24 | 2.147 | 0 | |
| | H4 | 2.479 | 0 | 0 | |
| | H5 | 1.24 | -2.147 | 0 | |
| | H6 | -1.24 | -2.147 | 0 | |
| $Ben(CH_4)_1$ | | | | | - 599 |
| Ligand | C1 | 0 | 0 | 3.421 | |
| | H1 | - .8989 | - .519 | 3.056 | |
| | H2 | .8989 | - .519 | 3.056 | |
| | H3 | 0 | 1.037 | 3.056 | |
| | H4 | 0 | 0 | 4.521 | |
| Ben $(CH_4)_2$ Configuration I | | | | | -1186 |
| Ligand 1 | C1 | 0 | 0 | 3.419 | |
| | H1 | - .8989 | - .519 | 3.054 | |
| | H2 | .8989 | - .519 | 3.054 | |
| | H3 | 0 | 1.037 | 3.054 | |
| | H4 | 0 | 0 | 4.519 | |
| Ligand 2 | C1 | 0 | 0 | -3.419 | |
| | H1 | - .8989 | - .519 | -3.054 | |
| | H2 | .8989 | - .519 | -3.054 | |
| | H4 | 0 | 0 | -4.519 | |
| Configuration II | | | | | -1177 |
| Ligand 1 | C1 | .695 | - .023 | 3.+-+ | |
| | H1 | .195 | - .905 | 3.0123 | |
| | H2 | 1.769 | - .0612 | 3.209 | |
| | H3 | .258 | .8907 | 3.0123 | |
| | H4 | .556 | - .018 | 4.531 | |

TABLE III
(continued)

| | Atom | X(Å) | Y(Å) | Z(Å) | Energy (cm$^{-1}$) |
|---|------|------|------|------|--------|
| Ligand 2 | C1 | -2.778 | .106 | 3.286 | |
| | H1 | -3.877 | .141 | 3.301 | |
| | H2 | -2.396 | .105 | 4.317 | |
| | H3 | -2.389 | .9836 | 2.750 | |
| | H4 | -2.449 | - .8102 | 2.774 | |

TABLE IV

The prominent peaks in the spectra of $Ben(C_2H_6)_1$ and $Ben(C_2H_6)_2$ in the region of $6_0^1$ (see figure 4).

| Species | Energy (vac $cm^{-1}$) | Energy relative to Ben $6_0^1(cm^{-1})$ | Energy relative to cluster $6_0^1(cm^{-1})$ | Assignment[a] |
|---|---|---|---|---|
| $Ben(C_2H_6)_1$ | 38551.3 | -57.2 | 0 | I $6_0^1$ |
| | 38568.0 | | 16.7 | I $6_0^1 V_0^1$ |
| | 38584.1 | | 32.8 | I $6_0^1 V_0^2$ |
| | 38601.6 | | 50.3 | I $6_0^1 V_0^3$ |
| | 38557.7 | -50.8 | 0 | II $6_0^1$ |
| | 38573.8 | | 16.1 | II $6_0^1 V_0^1$ |
| | 38589.4 | | 31.7 | II $6_0^1 V_0^2$ |
| | 38606.4 | | 48.7 | II $6_0^1 V_0^3$ |
| $Ben(C_2H_6)_2$ | 38555.6 | -52.9 | 0 | I $6_0^1$ |
| | 38560.5 | -48.0 | 0 | II $6_0^1$ |
| | 38568.7 | | 8.1 | II $6_0^1 A_0^1$ |
| | 38574.2 | | 13.6 | II $6_0^1 B_0^1$ |
| | 38578.2 | | 17.7 | II $6_0^1 V_0^1$ |
| | 38589.9 | | 29.4 | II $6_0^1 V_0^1 B_0^1$ |

a)
  A and B represent different vdW bending modes and V stands for the vdW symmetric stretch. I and II represent different geometries.

TABLE V

The prominent peaks in the spectra of $Ben(C_2H_6)_1$ and $Ben(C_2H_6)_2$ in the $0_0^0$ region (see figure 5).

| Species | Frequency (vac cm$^{-1}$) | Energy relative to $Ben(0_0^0$(cm$^{-1}$) | Energy relative to cluster $0_0^0$ | Assignment[a] |
|---|---|---|---|---|
| $Ben(C_2H_6)_1$ | 38039.0 | -45.4 | 0 | II $0_0^0$ |
| | 38047.3 | | 8.3 | II $A_0^1$ |
| | 38053.1 | | 14.1 | II $B_0^1$ |
| $Ben(C_2H_6)_2$ | 38040.2 | -44.2 | 0 | II $0_0^0$ |
| | 38048.4 | | 8.2 | II $A_0^1$ |
| | 38053.1 | | 12.9 | II $B_0^1$ |

a) Symbol notation is the same as in table IV.

## TABLE VI

The atomic positions for the minimum energy configurations of $Ben(C_2H_6)_1$
(see figure 6). The benzene coordinates are the same as in Table III.

| | Atom | X(Å) | Y(Å) | Z(Å) | Energy (cm$^{-1}$) |
|---|---|---|---|---|---|
| Configuration I | | | | | -654 |
| Ligand | C1 | 0 | 0 | 3.398 | |
| | C2 | 0 | 0 | 4.928 | |
| | H1 | - .8989 | - .519 | 3.033 | |
| | H2 | .8989 | - .519 | 3.033 | |
| | H3 | 0 | 1.037 | 3.033 | |
| | H4 | - .8989 | .519 | 5.293 | |
| | H5 | 0 | 1.037 | 5.293 | |
| | H6 | .8989 | .519 | 5.293 | |
| Configuration II | | | | | -778 |
| Ligand | C1 | - .173 | - .099 | 3.527 | |
| | C2 | 1.133 | .653 | 3.789 | |
| | H1 | - .639 | - .368 | 4.486 | |
| | H2 | .042 | - 1.013 | 2.954 | |
| | H3 | - .856 | .544 | 2.953 | |
| | H4 | .918 | 1.567 | 4.362 | |
| | H5 | 1.816 | .010 | 4.363 | |
| | H6 | 1.599 | .622 | 2.830 | |

## TABLE VII

The atomic positions for the minimum energy configurations of $Ben(C_2H_6)_2$ (see figure 7). The benzene coordinates are the same as in Table III.

| | Atom | X(Å) | Y(Å) | Z(Å) | Energy $(cm^{-1})$ |
|---|---|---|---|---|---|
| Configuration I | | | | | -988 |
| Ligand 1 | C1 | 0 | 0 | 3.396 | |
| | C2 | 0 | 0 | 4.926 | |
| | H1 | - .8989 | - .519 | 3.031 | |
| | H2 | .8989 | - .519 | 3.031 | |
| | H3 | 0 | 1.037 | 3.031 | |
| | H4 | - .8989 | .519 | 5.291 | |
| | H5 | 0 | - 1.037 | 5.291 | |
| | H6 | .8989 | .519 | 5.291 | |
| Ligand 2 | C1 | .001 | 0 | 8.346 | |
| | C2 | .001 | 0 | 9.876 | |
| | H1 | - .8979 | - .518 | 7.981 | |
| | H2 | .8999 | - .518 | 7.981 | |
| | H3 | .001 | 1.038 | 7.981 | |
| | H4 | .001 | - 1.038 | 10.241 | |
| | H5 | - .8999 | .518 | 10.241 | |
| | H6 | .8979 | .518 | 10.241 | |
| Configuration II | | | | | -1512 |
| Ligand 1 | C1 | - 2.624 | - 1.486 | 3.000 | |
| | C2 | - 3.177 | - 1.978 | 4.339 | |
| | H1 | - 3.318 | - 1.766 | 2.193 | |
| | H2 | - 1.643 | - 1.948 | 2.818 | |
| | H3 | - 2.516 | - .392 | 3.029 | |
| | H4 | - 4.257 | - 1.514 | 4.527 | |
| | H5 | - 3.284 | - 3.072 | 4.310 | |
| | H6 | - 2.482 | - 1.698 | 5.145 | |
| Ligand 2 | C1 | .374 | - .391 | 4.808 | |
| | C2 | .771 | .268 | 3.485 | |
| | H1 | .170 | - 1.458 | 4.636 | |
| | H2 | 1.196 | - .286 | 5.530 | |
| | H3 | - .528 | .098 | 5.203 | |
| | H4 | - .051 | .163 | 2.763 | |
| | H5 | 1.674 | - .220 | 3.091 | |
| | H6 | .976 | 1.336 | 3.657 | |

## TABLE VIII

The prominent peaks in the spectrum of $Ben(C_3H_8)_1$ and $Ben(C_3H_8)_2$ in the $6_0^1$ region (see figure 8).

| Species | Energy (vac $cm^{-1}$) | Energy relative to Ben $6_0^1$ ($cm^{-1}$) | Energy relative to cluster $6_0^1$($cm^{-1}$) | Assignment[a] |
|---|---|---|---|---|
| $Ben(C_3H_8)_1$ | 38536.5 | -72.0 | 0 | $6_0^1$ |
| | 38560.2 | | 23.7 | $6_0^1 v_0^1$ |
| | 38571.7 | | 35.2 | ? |
| | 38585.5 | | 49 | $6_0^1 v_0^2$ |
| | 38610.2 | | 73.7 | $6_0^1 v_0^3$ |
| | 38613.9 | | 77.4 | ? |
| $Ben(C_3H_8)_2$ | 38526.0 | -82.5 | 0 | $6_0^1$ |
| | 38538.0 | | 12.0 | $6_0^1 A_0^1$ |
| | 38543.9 | | 17.9 | $6_0^1 B_0^1$ |
| | 38548.7 | | 22.7 | $6_0^1 v_0^1$ |
| | 38566.4 | | 40.4 | $6_0^1 v_0^1 B_0^1$ |
| | 38571.7 | | 45.7 | $6_0^1 v_0^2$ |

a)
  A and B represent different vdW bending modes. V represents the vdW symmetric stretch.

## TABLE IX

The atomic positions for the minimum energy configurations of $Ben(C_3H_8)_1$ and $Ben(C_3H_8)_2$ (see figure 9). The axes and coordinates of benzene are the same as in Table III.

| | Atom | X(Å) | Y(Å) | Z(Å) | Energy $(cm^{-1})$ |
|---|---|---|---|---|---|
| $Ben(C_3H_8)_1$ | | | | | -1044 |
| Ligand | C1 | -1.121 | .7975 | 3.642 | |
| | C2 | .267 | .155 | 3.616 | |
| | C3 | .125 | -1.368 | 3.644 | |
| | H1 | -1.019 | 1.892 | 3.622 | |
| | H2 | -1.488 | .491 | 2.882 | |
| | H3 | -1.447 | .516 | 4.430 | |
| | H4 | .797 | .459 | 2.823 | |
| | H5 | .838 | .484 | 4.370 | |
| | H6 | 1.123 | -1.830 | 3.625 | |
| | H7 | - .324 | -1.532 | 2.884 | |
| | H8 | - .283 | -1.507 | 4.431 | |
| $Ben(C_3H_8)_2$ | | | | | -1643 |
| Ligand 1 | C1 | -1.132 | .791 | 3.637 | |
| | C2 | .256 | .148 | 3.611 | |
| | C3 | .114 | -1.375 | 3.639 | |
| | H1 | -1.030 | 1.885 | 3.617 | |
| | H2 | -1.499 | .484 | 2.877 | |
| | H3 | -1.458 | .509 | 4.425 | |
| | H4 | .786 | .452 | 2.818 | |
| | H5 | .827 | .477 | 4.365 | |
| | H6 | 1.112 | -1.837 | 3.620 | |
| | H7 | - .335 | -1.539 | 2.879 | |
| | H8 | - .294 | -1.514 | 4.426 | |
| Ligand 2 | C1 | - .229 | - .129 | 7.172 | |
| | C2 | - .170 | - .094 | 8.700 | |
| | C3 | 1.101 | .637 | 9.145 | |
| | H1 | -1.142 | - .654 | 6.853 | |
| | H2 | - .242 | .900 | 6.783 | |
| | H3 | .654 | - .658 | 6.784 | |
| | H4 | - .156 | -1.123 | 9.088 | |
| | H5 | -1.053 | .435 | 9.087 | |
| | H6 | 1.143 | .662 | 10.244 | |
| | H7 | 1.984 | .108 | 8.758 | |
| | H8 | 1.087 | 1.666 | 8.757 | |

TABLE X

The prominent peaks in the spectrum of $Ben(C_3H_8)_3$ in the $6_0^1$ and $0_0^0$ regions (see figure 10).

| Energy (vac $cm^{-1}$) | Energy relative to Ben feature ($cm^{-1}$) | Energy relative to cluster feature ($cm^{-1}$) | Assignment[a] |
|---|---|---|---|
| 38538.2 | -70.3 | 0 | I $6_0^1$ |
| 38558.7 | | 20.5 | I $6_0^1 B_0^1$ |
| | | | |
| 38549.1 | -59.4 | 0 | II $6_0^1$ |
| 38562.4 | | 13.3 | II $6_0^1 B_0^1$ |
| 38572.8 | | 23.7 | II $6_0^1 V_0^1$ |
| | | | |
| 38017.5 | -68.6 | 0 | I $0_0^0$ |
| 38037.8 | | 20.3 | I $B_0^1$ |
| | | | |
| 38027.3 | -58.8 | 0 | II $0_0^0$ |
| 38042.2 | | 14.9 | II $B_0^1$ |

a)
  B represents a vdW bending mode.  V represents the vdW symmetric stretch.  I and II stand for two different configurations.

## TABLE XI

The ratio of the solvent dimer binding energy to the benzene-solvent binding energy (BE).

| Solvent | Solvent dimer B.E.[a] $(cm^{-1})$ | Benzene-solvent[a] B.E. $(cm^{-1})$ | Ratio |
|---------|-----------------------------------|-------------------------------------|-------|
| methane | 277 | 599 | .47 |
| ethane | 503 | 778 | .65 |
| propane | 789 | 1044 | .75 |

a)
   All values are calculated by computer modeling of the complex.

FIGURE CAPTIONS

## FIGURE 1

Mass selective absorption spectra of $\text{Ben}(CH_4)_1$, $\text{Ben}(CH_4)_2$ and $\text{Ben}(CH_4)_3$ in the region of the $6_0^1$ transition of benzene. The energy scale is relative to the Ben $6_0^1$ transition ($38608.5$ cm$^{-1}$). Peak positions are given in Table II. The peak positions for $\text{Ben}(CH_4)_3$ are not tabulated.

## FIGURE 2

Mass selective absorption spectrum of $\text{Ben}(CH_4)_2$ in the region of $0_0^0$ transition of benzene. The energy scale is relative to the $\text{Ben}(0_0^0$ ($38086.1$ cm$^{-1}$). The presence of an origin for configuration II of $\text{Ben}(CH_4)_2$ (ca. $\jmath8042$ cm$^{-1}$) indicates that the 3-fold axis of benzene is destroyed in this geometry.

## FIGURE 3

Minimum energy configurations of $\text{Ben}(CH_4)_1$ and $\text{Ben}(CH_4)_2$. Atomic positions are given in Table III. Note that the 3-fold axis of benzene is preserved in $\text{Ben}(CH_4)_1$ and geometry I of $\text{Ben}(CH_4)_2$, but not in geometry II of $\text{Ben}(CH_4)_2$.

FIGURE 4

Mass selective absorption spectra of $Ben(C_2H_6)_1$ and $Ben(C_2H_6)_2$ in the $6_0^1$ region of benzene. The energy scale is relative to the Ben $6_0^1$ (38608.5 $cm^{-1}$). The peak position indicated are tabulated in Table IV.


FIGURE 5

Mass selective absorption spectra of $Ben(C_2H_6)_1$ and $Ben(C_2H_6)_2$ in the $0_0^0$ region of benzene. The energy scale is relative to the Ben $0_0^0$ (38086.1 $cm^{-1}$). Note that only configuration II exhibits an origin and vdW bends. Peak positions are given in Table V.


FIGURE 6

Minimum energy geometries of $Ben(C_2H_6)_1$. Atomic positions are given in Table VI. Note that in geometry I the 3-fold axis of benzene is preserved, but in II it is not.


FIGURE 7

Minimum energy geometries of $Ben(C_2H_6)_2$. Atomic positions are given in Table VII. Note that geometry I preserves the 3-fold symmetry of benzene, but geometry II does not.


FIGURE 8

Mass selective absorption spectra of $Ben(C_3H_8)_1$ and $Ben(C_3H_8)_2$ in the $6_0^1$ region of benzene. The energy scale is relative to the Ben $6_0^1$(38608.5 $cm^{-1}$). The peak positions indicated are tabulated in Table VIII.

FIGURE 9

Minimum energy geometries of $Ben(C_3H_8)_1$ and $Ben(C_3H_8)_2$. Atomic

positions are given in Table IX. Note that the 3-fold symmetry of

benzene is nearly preserved by the atoms closest to benzene for both

species.


FIGURE 10

Mass selective absorption spectrum of $Ben(C_3H_8)_3$ in the $6_0^1$ and

$0_0^0$ regions. The energy scales are relative to the Ben $6_0^1$ (38608.5

$cm^{-1}$) and the Ben $0_0^0$ (38086.1 $cm^{-1}$). Peak positions are given

in Table X. Note that both geometries of $Ben(C_3H_8)_3$ destroy the

3-fold symmetry of benzene.

$6^1_0$

Ben$(CH_4)_1$

I

II

Ben$(CH_4)_2$

Ben$(CH_4)_3$

-100

0

RELATIVE ENERGY (WAVENUMBERS)

$O_0^0$

$Ben(CH_4)_2$

-100                            0

RELATIVE ENERGY (WAVENUMBERS)

I

II

$6^1_0$

Ben $(C_2H_6)_1$

I

II

Ben $(C_2H_6)_2$

II

I

- 100

0

RELATIVE ENERGY (WAVENUMBERS)

$O_0^0$

Ben$(C_2H_6)_1$

Ben$(C_2H_6)_2$

-100                                              0

RELATIVE ENERGY (WAVENUMBERS)

II

I

II

H

$6^1_0$

Ben$(C_3H_8)_1$

Ben$(C_3H_8)_2$

-100                                    0

RELATIVE ENERGY (WAVENUMBERS)

$6_0^1$

I  II

$Ben(C_3H_8)_3$

$0_0^0$

I  II

-100                                    0

-100                                    0

RELATIVE ENERGY (WAVENUMBERS)

DTIC

END

4-86